actuators

Article

Evaluation of Switching Power Amplifier Topology for Active Magnetic Bearings

Kezhen Yang [1], Yefa Hu [2], Xinhua Guo [2], Jian Zhou [1] and Huachun Wu [2,*]

[1] School of Mechanical & Electronic Engineering, Wuhan University of Technology, Wuhan 430070, China; yangkezhen@whut.edu.cn (K.Y.); whutdrz@whut.edu.cn (J.Z.)
[2] Hubei Provincial Engineering Technology Research Center for Magnetic Suspension, School of Mechanical & Electronic Engineering, Wuhan University of Technology, Wuhan 430070, China; huyefa@whut.edu.cn (Y.H.); xguo@whut.edu.cn (X.G.)
* Correspondence: whc@whut.edu.cn

Abstract: Active magnetic bearings (AMBs) have led to great progress in the field of rotating machinery due to their many advantages, such as their non-contact and non-lubrication properties. As the key component of an AMB actuator, the switching power amplifier has an important impact on the performance of magnetic bearings and rotating machinery. In this paper, the topologies of switching power amplifiers for AMBs are introduced. The traditional half-bridge topology and two newly proposed topologies—the three-phase-half-bridge and neutralized-sharing-bridge topology—are analyzed and discussed. The volume, current output performance and cost of the power amplifier with different topologies are comprehensively evaluated, providing a theoretical basis and guidance for the selection and design of the topology of switching power amplifiers for AMBs under different conditions.

Keywords: electromagnetic actuators; active magnetic bearings; switching power amplifier; topology

Citation: Yang, K.; Hu, Y.; Guo, X.; Zhou, J.; Wu, H. Evaluation of Switching Power Amplifier Topology for Active Magnetic Bearings. *Actuators* **2021**, *10*, 131. https://doi.org/10.3390/act10060131

Academic Editors: Jose Luis Sanchez-Rojas and Tatiana Minav

Received: 11 May 2021
Accepted: 10 June 2021
Published: 13 June 2021

1. Introduction

Active magnetic bearings (AMBs) use an electromagnetic actuator to generate a controllable electromagnetic force to support a high-speed rotating rotor without any contact [1]; Figure 1 presents the stator model of an AMB. The non-contact supporting characteristics of AMBs give them the advantages of no wear, no lubrication, a low operating cost, long life and so on [2], promoting the development of maglev high-speed motors, maglev flywheel batteries and other equipment to achieve ultra-high speed and a high power density; they are also increasing widely used in equipment in special environments, such as molecular pumps and satellite control moment gyroscopes.

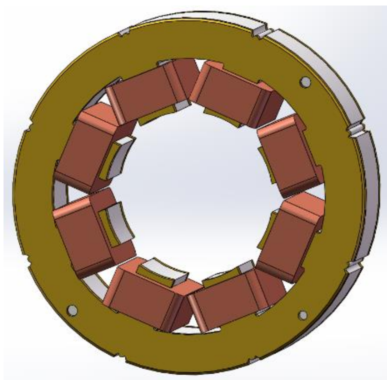

Figure 1. Three-dimensional model of an AMB stator.

The AMB system has negative displacement stiffness, which makes it an open-loop unstable system [3]. To realize the stable operation of the AMB system, an appropriate controller must be implemented to realize closed-loop feedback control. Figure 2 illustrates the principle of a radial AMB with two vertical axes. For each axis, the displacement sensor is used to detect the rotor displacement off the center in real-time and feed it back to the controller, and the controller calculates and obtains the reference current signal. The power amplifiers magnify the reference current signals, which are in the form of the voltage, into two real expected currents, which excite the two electromagnets to produce the desired electromagnetic force and attract the rotor back to the center position. According to the closed-loop control process, the AMB system can be divided into four key parts: the sensor, the controller, the power amplifier and the electromagnet. The performance of the power amplifier determines the performance of the whole AMB system. Only with an efficient and reliable power amplifier can the AMB system achieve stable suspension and meet the requirements of the ISO standard [4].

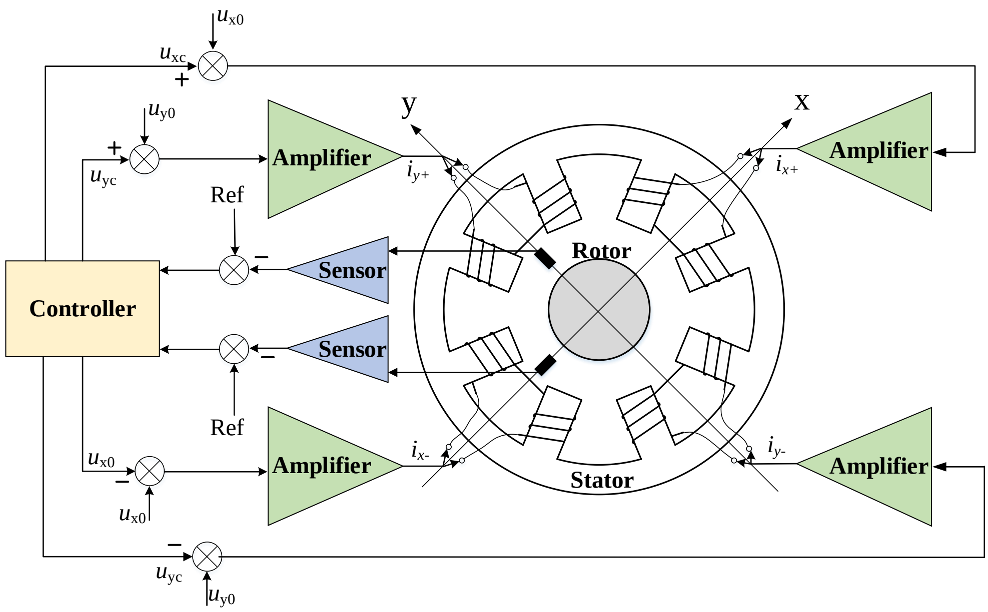

Figure 2. Basic principle of a radial AMB.

Due to the fundamental role of power amplifiers in the AMB system, many scholars have studied them. A linear power amplifier was used in AMBs in the early stage [5], but power devices working in the linear region consume a great deal of power, so they have been substituted with switching power amplifiers (SPAs). Regarding the accuracy characteristic of the output current of SPAs, Xin Cheng et al. [6] studied the main factors affecting the inherent current ripple. To reduce the current ripple and improve the current response rate simultaneously, Hsin-Lin Chiu et al. [7] designed a dual-mode power drive as the hybrid power amplifier under the consideration of both the transient and steady state of the AMB system and showed its superiorities in their experiment. Yuan Ren et al. [8] proposed a current predictive control method based on proportional–differential current-sensing resistor networks to solve the problem of digital control delay in traditional linear predictive control in SPAs, which improved the current tracking accuracy and reduced the current ripple. Jiancheng Fang et al. [9] also proposed a self-adaptive phase-led compensation strategy based on an unsymmetrical current sampling resistance network to solve the problem of phase lag in SPA, which improved the system stability and the static and dynamic performance. However, these articles mainly studied the current control strategy of an AMB system and the output current characteristics of SPAs, and the research objects were merely the traditional full-bridge or half-bridge topology power amplifiers.

An SPA for a magnetic bearing is a typical power electronic converter, the topology of which has an important influence on its performance and application. Therefore, some scholars have proposed and studied new topologies of SPAs. Dong Jiang et al. [10] studied a reduced switch converter for AMBs which decreases the number of components and analyzes the modulation method and control strategy. Then, considering the multi-axis drive requirements of the AMB system, Dong Jiang [11] further proposed a shared-bridge drive with reversed direction and designed an SPA with a redundant structure with this topology. Jie Zhou [12] designed a five-phase six-leg topology SPA for a five degree of freedom (DOF) AMB system and proposed the one-cycle current control algorithm, which effectively reduced the output current ripple.

However, these studies have mainly focused on reducing the number of switches and verifying the feasibility of basic functions of SPAs with a novel topology. Hu Yefa et al. [13] evaluated different topologies but gave guidance of SPA topologies selection only in case of different coil pair arrangements and bias current distributions. There is a lack of a comprehensive analysis and evaluation of SPAs, especially in terms of the analysis of the cost, accuracy, and rapidity of its output current. Therefore, this paper analyzes and discusses several traditional and novel topologies of SPAs and comprehensively compares three topologies with strong representativeness and high practical value, including half-bridge, three-phase-half-bridge, and neutralized-sharing-bridge designs. This paper makes a complete evaluation of the three topologies in terms of the volume, current output performance, and cost of SPAs, which can provide theoretical guidance and reference for the selection and design of topology for SPAs for AMBs in different situations. This work is conducive to the promotion and widespread application of magnetic bearing technology.

2. Topologies of AMB Amplifiers

The SPAs of AMBs can achieve an increase or decrease in the coil current by controlling the opening and closing of the switches. In terms of topology, the bridge structure is generally adopted, and other kinds of topologies are modified based on the full-bridge topology. Figure 3 displays the full-bridge topology of an SPA, which has the capability of controlling the current of one coil, and the coil is simplified as a resistance and inductance series connection. The controller outputs pulse width modulation (PWM) waves with certain duty cycles to control the opening or closing of the four switches and adjust the coil current in real-time. Specifically, assuming that the coil current direction is from left to right, if S_1 and S_4 are opened at the same time, the positive voltage $+V_{dc}$ on the coil increases the coil current; if S_2 and S_3 are opened, the coil current decreases due to the negative voltage ($-V_{dc}$); and if S_1, S_3 or S_2, and S_4 are opened simultaneously, the coil current freewheels and slowly decreases due to the energy consumption on the equivalent resistance of the coil. Therefore, as long as four switches are controlled with an appropriate control method, the coil current can track the reference current signal with high performance.

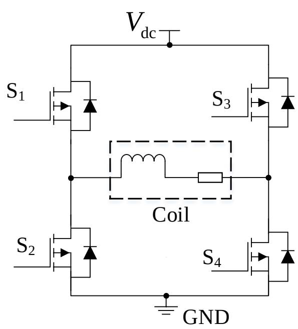

Figure 3. Full-bridge topology of an SPA.

A bridge circuit can control the current of one coil, but is not sufficient to control the motion of the rotor in one DOF. This is because the electromagnetic force has a strong nonlinear characteristic, so an AMB generally adopts differential control with two coils controlling one DOF motion [14], as shown in Figure 2, and the electromagnetic force can be linearized when the rotor is near the center position. Therefore, the complete suspension of the rotor requires two radial AMBs, as shown in Figure 1. The axial DOF can be limited by the coupling that transmits the torque of the motor, which consequently creates a four DOF AMB, or the axial DOF is constrained by an axial thrust AMB, which forms a five DOF AMB. For a four DOF AMB, there are four DOF of motion to be limited, which requires that the amplifier has at least eight full-bridge circuits, as presented in Figure 4; thus, 32 switches and corresponding isolation drive circuits are required.

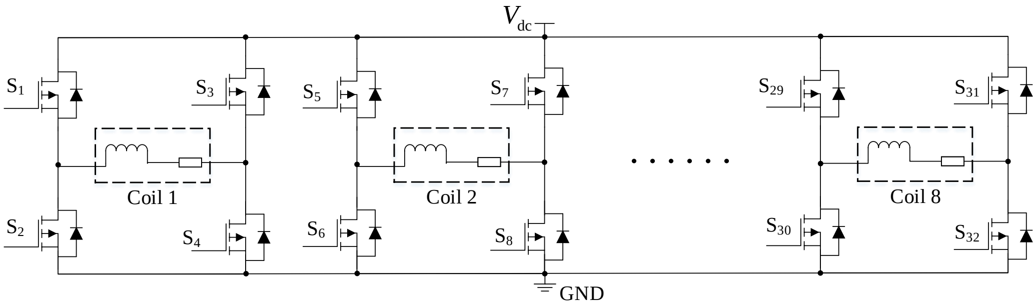

Figure 4. Full-bridge circuit of the SPA for a four DOF AMB.

A large number of components increases the volume and weight of the SPA as well as the possibility of the failure of the whole SPA, but also provides motivation and basic conditions for the optimization of the topology. To fairly evaluate an SPA with different topologies, the basic parameters of the SPA studied in this paper are kept consistent. The DC bus voltage V_{dc} is 150 V, the switching frequency f_{s} equals 20 kHz, and the coil resistance R and inductance L are 2.1 Ω and 5.3 mH respectively.

2.1. Half-Bridge Topology

The SPA with a full-bridge topology is mainly used in hybrid magnetic bearings because this demands an SPA that can provide bidirectional current [15]. The SPA with a half-bridge topology is widely applied in AMBs, as shown in this paper. The half-bridge topology, as shown in Figure 5, is the most mature topology of SPAs for AMBs. Because AMBs adopt differential control, the currents of two coils controlling one DOF of motion are equal to the bias current i_0 with the addition and subtraction of the control current i_{c}, respectively. Moreover, the coil current will only change near the bias current i_0, so the half-bridge topology SPA, which only provides unidirectional current, can completely meet the requirements for AMBs. A half-bridge topology SPA can realize current control of one coil only by two switches, S_1 and S_2, and two diodes, D_1 and D_2, which saves half of the switches and corresponding isolated drive circuits. However, the SPA for the four DOF AMB still needs at least eight half-bridge circuits, as shown in Figure 6, making a total of 16 switches. The number of components is still very large, and the topology has the potential for further optimization.

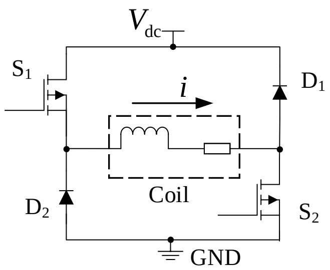

Figure 5. Half-bridge topology of an SPA.

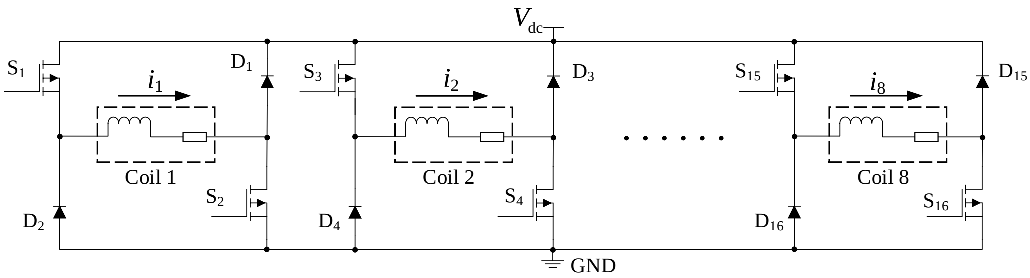

Figure 6. Half-bridge circuit of the SPA for the four DOF AMB.

2.2. Three-Phase-Half-Bridge Topology

To reduce the cost and complexity of the SPA, referring to the topology of the switched reluctance motor drive circuit, the three-phase-half-bridge topology SPA for AMBs is proposed [16]. Two half-bridges controlling two coils of one DOF are combined to develop the three-phase-half-bridge by sharing a phase leg, as shown in Figure 7. Only three switches are necessary to control the motion of one-DOF. For the four DOF AMB system, 12 switches are needed, and the number of components is reduced. The ground of the switch at the upper end of the bridge is floating; thus, it has to be driven by an isolated power supply, and the switches at the lower end can only share one power supply. Although the positions of switches and diodes can be interchanged in theory, switches S_1 and S_2 of phase legs on both sides are arranged at the lower end, while the switch S_0 of the middle phase leg is arranged at the upper end, reducing the use of the isolated power supply. In addition, because the middle phase leg is shared by two coils, its working characteristics are related to both coils and need further discussion.

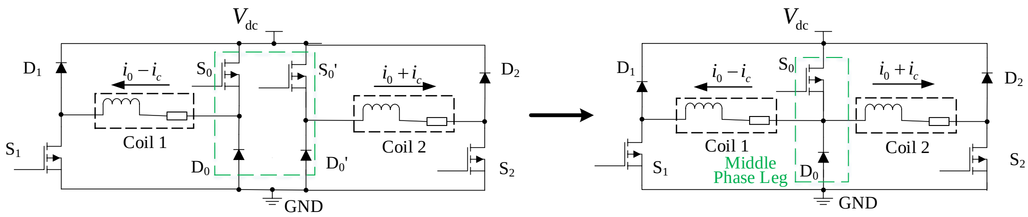

Figure 7. Three-phase-half-bridge topology of the SPA.

The middle phase leg is the main circuit, so the current that the components need to withstand is the sum of the currents of the two coils. The two coils are differentially controlled, so the current on the middle phase leg is constantly twice the bias current, which is exactly the maximum current of the phase legs on either side in the most extreme case. Thus, the selection and design of the middle switch S_0 can be consistent with the switches S_1 and S_2 on both sides, except that the heat dissipation needs special consideration [13]. The consistency of components is of great significance for the large-scale application of the three-phase-half-bridge topology SPA in the industrial field.

The control method for the middle phase leg switch S_0 can be classified into coupling control and decoupling control [10]. The duty cycles δ_1 and δ_2 of switches S_1 and S_2 on both sides are related to the coil current of the corresponding side, which is determined by the current controller after calculating the deviation between the coil current and the reference value, while the duty cycle of the middle switch S_0 is δ_0. When coupling control is adopted, the duty cycle δ_0 of switch S_0 is the sum of duty cycles of switches S_1 and S_2:

$$\delta_0 = \delta_1 + \delta_2 \tag{1}$$

Thus, each middle switch of the respective three-phase-half-bridge circuit needs a separate PWM signal to be controlled independently. The coupling control method increases not only the computational burden of the current controller but also the complexity of the SPA. Therefore, decoupling control is generally used in practical applications [10]. When decoupling control is adopted, the middle switch S_0 has a constant 50% duty cycle, so the average voltages on the two coils are:

$$\begin{array}{r} V_{C1} = (\delta_1 - 0.5)\, V_{dc},\, 0 < \delta_1 < 1 \\ V_{C2} = (\delta_2 - 0.5)\, V_{dc},\, 0 < \delta_2 < 1 \end{array} \quad (2)$$

Therefore, the average voltages on the coils change continuously between $-0.5V_{dc}$ and $+0.5V_{dc}$, which affects the output performance of SPA. A detailed analysis and comparison is given in Section 3.2.

2.3. Neutralized-Sharing-Bridge Topology

For a multi-axis AMB system, the middle phase legs of every three-phase-half-bridge play an identical role, and the duty cycles are the same, at 50%. Therefore, the middle phase legs controlling different axes can be integrated into a single main shared phase leg, as shown in Figure 8, which forms an integrated-shared-bridge topology [11]. A total of nine switches are required to realize the control of the four DOF AMB system. However, the current direction of each coil is equal; according to Kirchhoff current law, the current I on the integrated shared phase leg is the sum of the currents of eight coils:

$$I = i_1 + i_2 + i_3 + i_4 + i_5 + i_6 + i_7 + i_8 \quad (3)$$

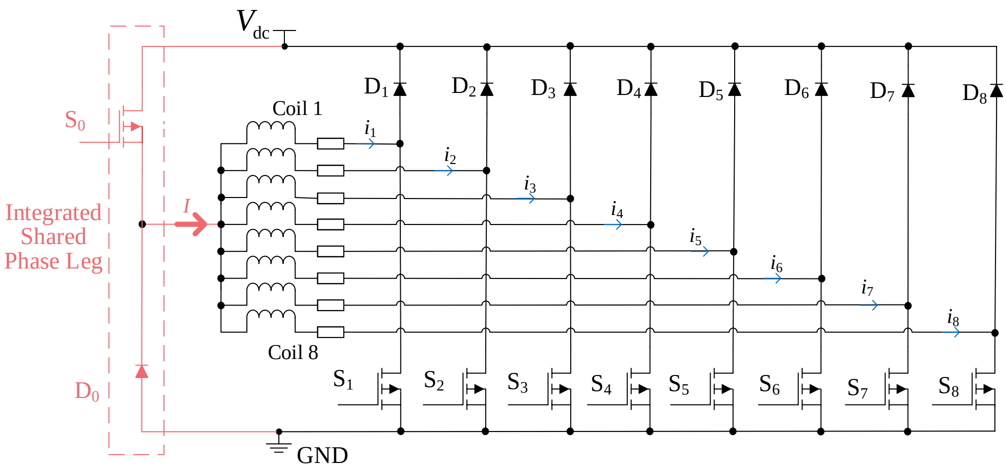

Figure 8. Integrated-sharing-bridge topology of the SPA for the four DOF AMB.

The switch S_0 and diode D_0 on the integrated shared phase leg have to withstand a large current; consequently, their selection needs special consideration. Heat dissipation also needs careful design and the operating life may even be reduced. This will have a serious impact on the performance and stability of the whole amplifier and even the AMB system, so this topology is not considered in the current design and application.

Since the current direction of the coil does not affect the performance of the AMB, half of the coils can be reversed to develop a neutralized-sharing-bridge topology, as presented in Figure 9. The coils are divided into two groups: the current of the first group of coils (coil 1 to 4) flows out of point O, and the current of the second group of coils (coil 5 to 8) flows into point O. According to Kirchhoff's current law, the current on the neutralized shared phase leg is the difference of the currents of the two groups, instead of the sum:

$$I = (i_1 + i_2 + i_3 + i_4) - (i_5 + i_6 + i_7 + i_8) \quad (4)$$

To fully reduce the current on the neutralized shared phase leg, two coils controlling one axis are arranged in the same group [13]. One group of coils is composed of two pairs of coils which control two DOFs, and the current I_N on the neutralized shared phase leg is obtained by subtracting the bias current of the two groups of coils. Moreover, when the bias current of each axis coil is designed to be equal, the current I_N on the neutralized shared leg is not only no more than the coil current, but even almost equal to zero. The current pressure of the components on the neutralized shared phase leg is greatly relieved, and the reliability of SPA is improved, which makes it meaningful to use only one shared leg.

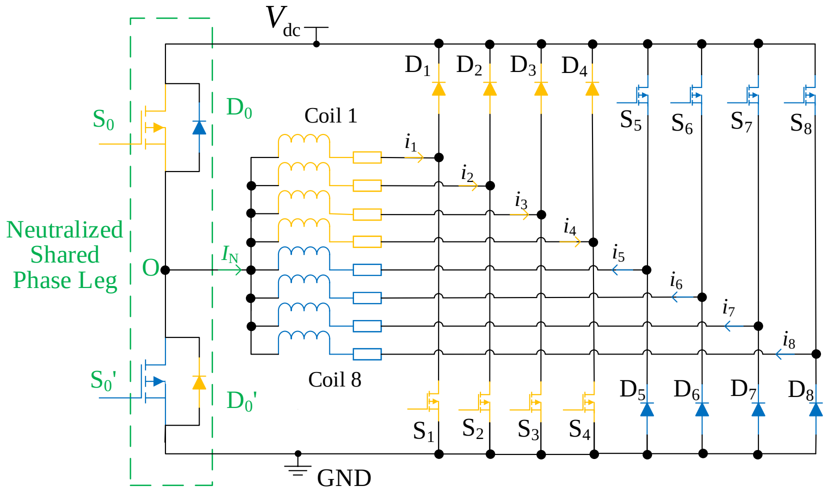

Figure 9. Neutralized-sharing-bridge topology of the SPA for the four DOF AMB.

3. Analysis and Comparisons of Topologies

3.1. Comparison of SPA Volume

From the half-bridge to three-phase-half-bridge and then to neutralized-sharing-bridge topology, the degree of bridge integration increases. This development of topology aims to make full use of components, so the number of switches required decreases. The complexity of SPA is reduced, and the volume is naturally reduced. Moreover, topology variation does not demand stricter performance from the switches, which makes it more meaningful to reduce the number of switches. If only the number of switches is considered, it is obvious that the neutralized-sharing-bridge topology is the best option. Nevertheless, the switches in the second group are all on the upper end of the bridge, and additional isolation power is needed, which would introduce extra components and increase the volume. Table 1 shows comparisons of the specific numbers of switches, diodes and isolated power suppliers employed in these three topologies.

Table 1. Comparisons of component numbers with three topologies for the four DOF AMB.

Topology	Switches	Diodes	Isolated Power Suppliers
Half-bridge	$4 \times 4 = 16$	$4 \times 4 = 16$	$4 \times 2 + 1 = 9$
Three-phase-half-bridge	$3 \times 4 = 12$	$3 \times 4 = 12$	$4 + 1 = 5$
Neutralized-sharing-bridge	$2 \times 4 + 2 = 10$	$2 \times 4 + 2 = 10$	$4 + 2 = 6$

Therefore, compared with the number of components in the SPA for the four DOF AMB with a half-bridge topology, the numbers with three-phase-half-bridge and neutralized-sharing-bridge topologies are greatly reduced, and so are the weight, volume and complexity of the SPA. However, the difference between the three-phase-half-bridge and neutralized-sharing-bridge topology is very small, and each has its advantages. Both need to be compared in detail in the actual application process. Nonetheless, if the SPA for the five DOF AMB is designed, along with the same number of isolated power suppliers, the number of components in the neutralized-sharing-bridge topology circuit will be distinctly smaller than that in the three-phase-half-bridge topology circuit (the numbers of switches and diodes will both decline by three), and the weight and volume of the bridge circuit reduce by 20%. Based on this condition, the advantages of decreasing the number of components with the neutralized-sharing-bridge topology are fully shown, promising broad application prospects in aerospace and other volume-sensitive and mass-sensitive fields.

3.2. Comparisons of Output Performance

The SPA magnifies the reference current signal to excite the coil. To ensure the performance of the SPA output current, current feedback control is generally introduced, and the output current is required to be fast, accurate, and stable as it follows the reference current signal. The ordinary proportional–integral (PI) control is generally adopted to acquire an output current with high stability, but without considering the characteristics of SPA. Thus, when the current output performance of an SPA is studied, the accuracy and rapidity of the output current, which is inextricably related to the characteristics of SPA, should be given close attention. In addition, MATLAB/Simulink is used to simulate different topologies in the following analysis.

3.2.1. Comparison of Current Ripple

The accuracy of the output current of SPA is represented by ripple. It is the inherent current fluctuation of SPA in the switching period, which cannot be eliminated, but it has an important influence on the suspension accuracy of the magnetically levitated rotor. Therefore, it is expected that the SPA output current will have the minimum ripple. Figure 10 displays the current control loop with a half-bridge topology amplifier. The three-level modulation method is implemented with a logic circuit, which can greatly reduce the ripple [6] and avoid it being affected by DC voltage. The ripple Δi is expressed as:

$$\Delta i = \Delta V/(2 f_s L) \approx (V_{on} + V_D + V_R)/(2 f_s L) \quad (5)$$

where V_{on} and V_D are the conduction voltage drop of the switch and free-wheeling diode, respectively, V_R is the voltage on the equivalent resistance of the coil, f_s is the switching frequency of the SPA, and L is the equivalent inductance of the coil. For an AMB system, the switching frequency f_s and coil inductance L have been determined at the beginning of the design, so the ripple is not related to the denominator, and, in this simulation, the switching frequency f_s and coil inductance L are 20 kHz and 5.3 mH, respectively, as presented in Section 2. In Equation (5), the numerator on the right side is the voltage drop ΔV in the free-wheeling loop, which is usually very small. Thus, the ripple with the half-bridge topology is small and not affected by the DC bus voltage. The basic parameters in Section 2 are used to simulate the current loop with a half-bridge SPA, and a constant 4 A current excitation is generated for the coil. The stable current is depicted in Figure 11, and the ripple is about 50 mA.

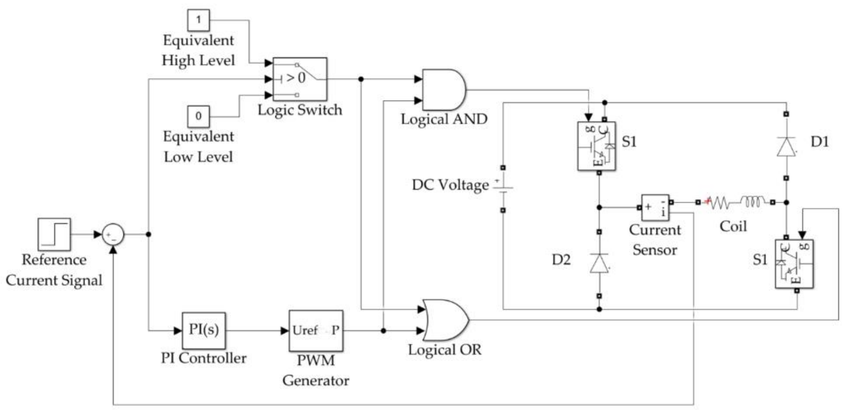

Figure 10. Current control loop with a half-bridge SPA.

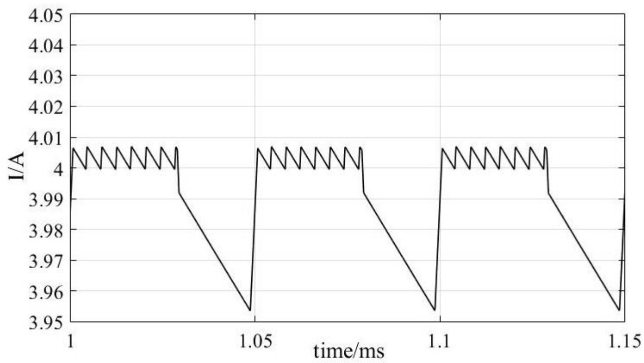

Figure 11. Current ripple of the SPA with a half-bridge topology.

For the amplifier with a three-phase-half-bridge topology, the method of in-phase modulation [10] can be used and a smaller current ripple is obtained; the ripple is also expressed by Equation (5). The current loop with a three-phase-half-bridge topology in Figure 12 is simulated, and the currents exciting both coils are constant at 4 A. When the current is stable, as shown in Figure 13, the ripple is around 80 mA. Although the ripple is larger than that with half-bridge amplifier, it is still within 100 mA and at a lower level.

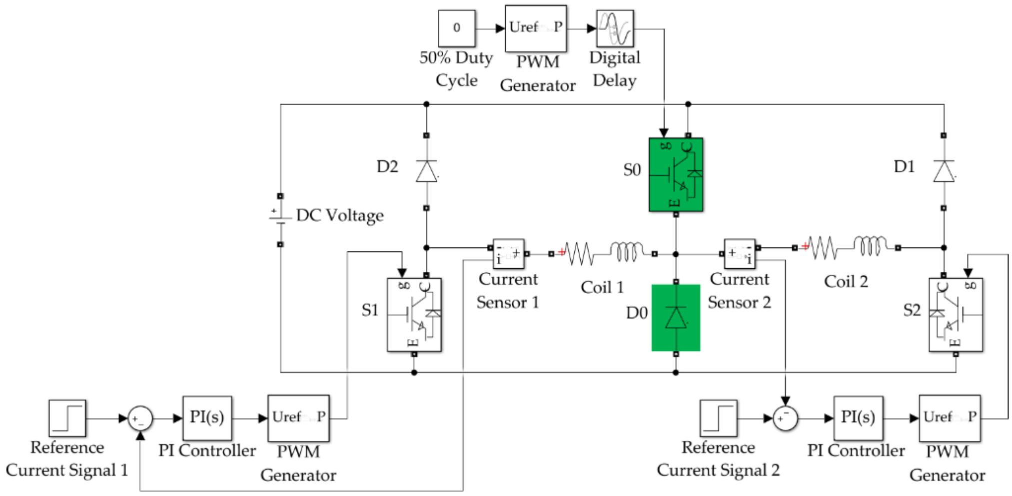

Figure 12. Current control loop with a three-phase-half-bridge SPA.

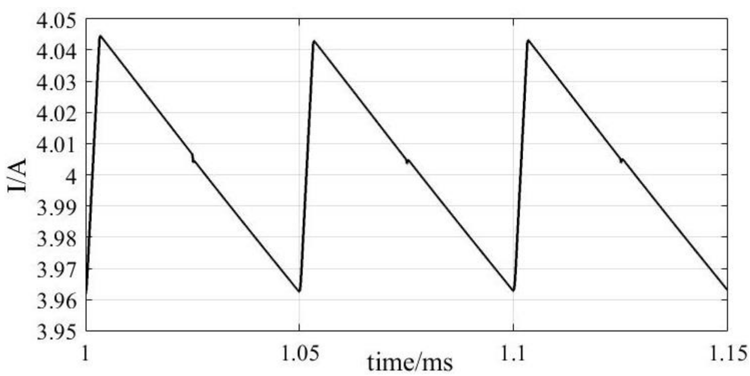

Figure 13. Current ripple of the SPA with a three-phase-half-bridge topology.

Similarly, the in-phase modulation method can also be used in the SPA with a neutralized-sharing-bridge topology. In contrast to the three-phase-half-bridge topology SPA, there may be a variety of situations in the free-wheeling loop structure of the neutralized-sharing-bridge topology amplifier. However, they are also merely a combination of switches, free-wheeling diodes and coils, and the loop voltage drop is still very small, so the output current ripple is small. The SPA with a neutralized-sharing-bridge topology as shown in Figure 14 is simulated, where the current controller, current sensor, and other four circuits are omitted due to space limitations. The amplifier outputs a constant current of 4 A for all coils. The current of one coil is shown in Figure 15, and the ripple is approximately 60 mA. When the current increases, the voltage on the coil is V_{DC}, so the slope is very large; when the current drops, the voltage drop of the free-wheeling loop is very low, and so the decline is slow and the decline slope will change slightly due to the change of the free-wheeling loop.

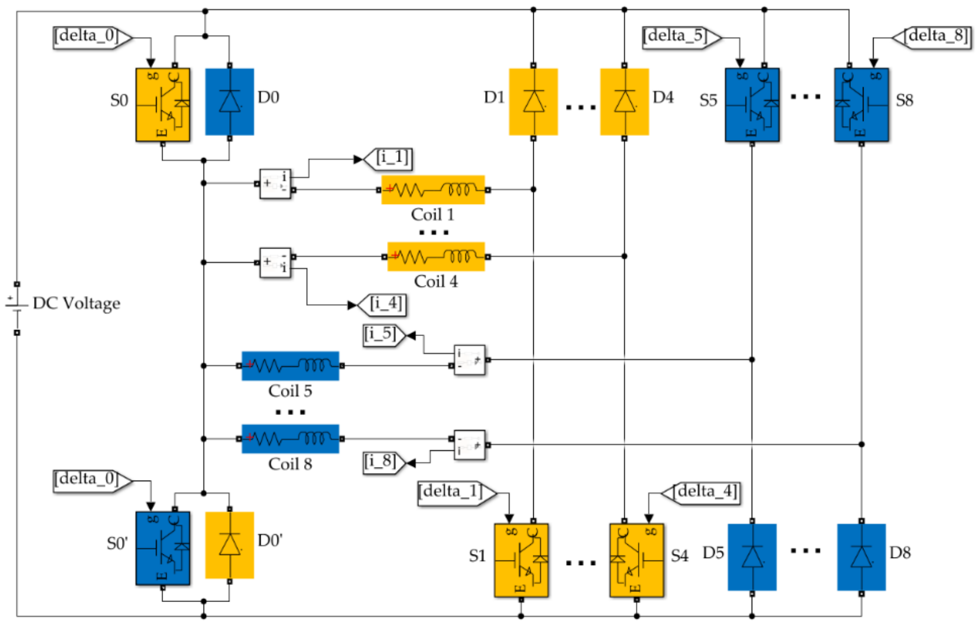

Figure 14. Current control loop with a neutralized-sharing-bridge SPA (with controller omitted).

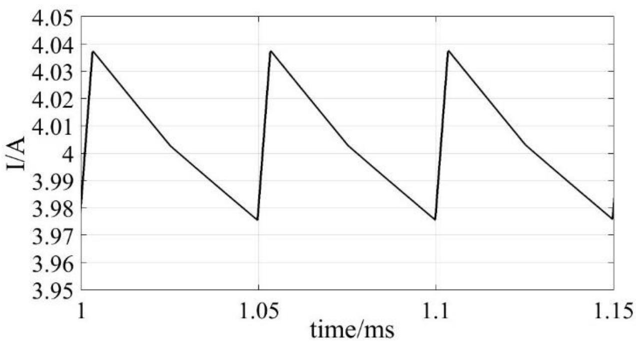

Figure 15. Current ripple of the SPA with a neutralized-sharing-bridge topology.

Therefore, current ripple, as an inherent property of an SPA, exists in the output current of an amplifier with any topology, but the three topologies of SPAs can result in a very small ripple through an appropriate modulation method, and the difference in the output current ripple is small.

3.2.2. Comparison of Output Current Response Rate

The coil of an AMB is an inductive load. The output current response rate dI/dt of the AMB coil is an important index to measure the performance of an SPA, which represents the rapidity of the output current following the reference current signal. A higher current response rate indicates that the SPA has a higher control bandwidth and better dynamic performance. The output current response rate of SPA can be expressed by Equation (6):

$$\mathrm{d}I/\mathrm{d}t = (V_\mathrm{C} - V_\mathrm{R})/L \approx V_\mathrm{C}/L \tag{6}$$

where V_C is the voltage on the coil, and the coil inductance L is determined at the initial design stage, so the output current response rate is proportional to the voltage V_C on the coil. When the half-bridge topology is adopted, the voltage on the coil is $\pm V_\mathrm{dc}$; however, when the three-phase-half-bridge or neutralized-sharing-bridge topology is adopted, the voltage on the coil is $\pm 0.5\ V_\mathrm{dc}$, half of that with half-bridge, so its current response rate is only half of that of the half-bridge topology SPA. Under the same parameters given in Section 2, the SPAs with three topologies are simulated. The step reference signal is input at 1 ms, and the amplifiers are controlled to output 4 A of current. The time at which the coil current reaches the reference value is compared, as demonstrated in Figure 16.

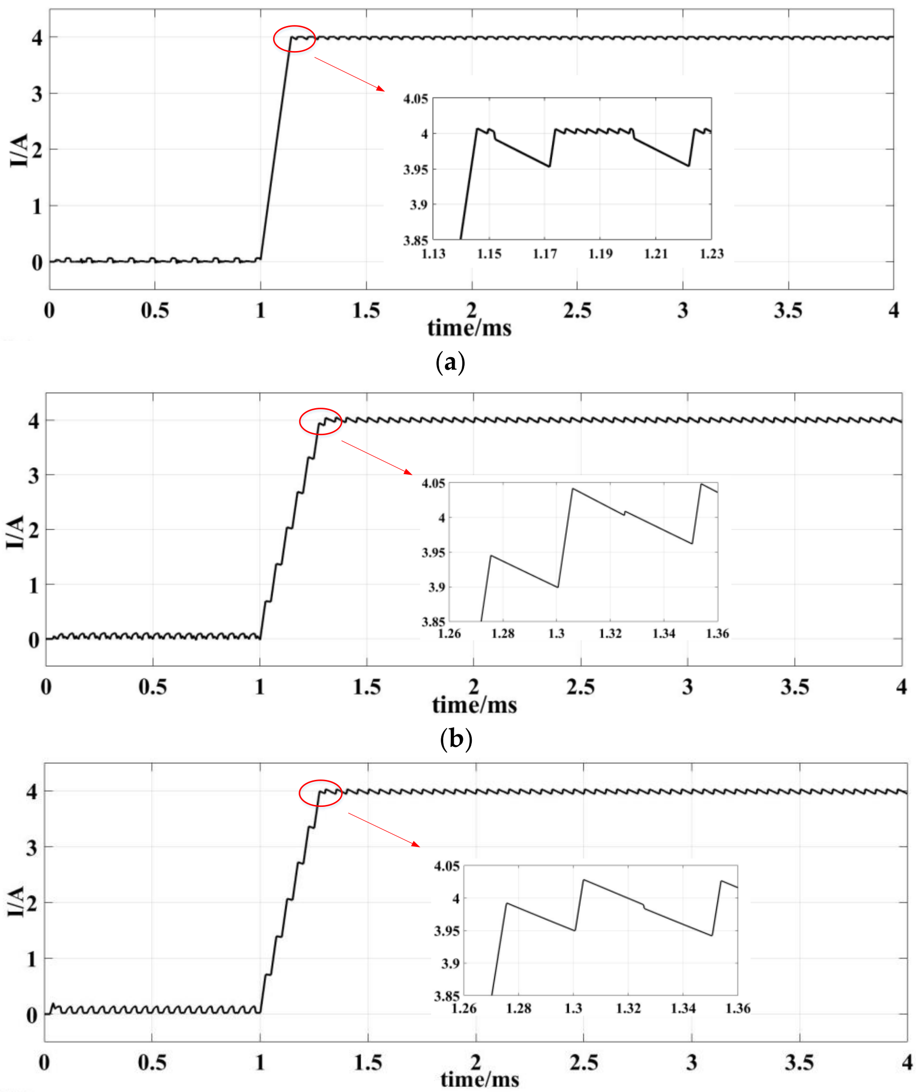

(**a**)

(**b**)

(**c**)

Figure 16. Current rise curves of SPAs with (**a**) half-bridge topology, (**b**) three-phase-half-bridge topology, and (**c**) neutralized-sharing-bridge topology.

According to the simulation results, the coil current of the half-bridge topology SPA continues to rise, taking approximately 0.14 ms to increase from 0 A to 4 A. However, for the three-phase-half-bridge topology and the neutralized-sharing-bridge topology, the middle leg is not in operation for 50% of the time, and the increase in the coil current is discontinuous. It takes roughly 0.28 ms to increase from 0 A to 4 A, which is twice as much as that of the half-bridge topology.

Therefore, the half-bridge topology has a faster output current response rate and wider current control bandwidth, which has outstanding advantages in the stability control of ultra-high-speed magnetically levitated rotors.

3.3. Comparison of SPA Cost

On the basis of meeting the basic performance requirements, the cost of SPAs with different topologies should also be deliberately considered in the design of an AMB system. The numbers of components of the three-phase-half-bridge topology and neutralized-sharing-bridge topology are reduced, and the components on the shared leg need no special consideration, so they have more advantages in cost than the half-bridge topology.

In industrial mass production in particular, cost is the first consideration. In fact, the structure of a three-phase-half-bridge topology SPA is very similar to that of a three-phase inverter. The three-phase inverter has a wide range of applications in the industrial field, from motor drive to high-end applications, such as motion control and robotics; thus, various specifications of three-phase inverters are produced in very large unit quantities [17]. Using a three-phase inverter as a three-phase-half-bridge circuit in AMBs can result in a low-cost, standardized, high-integration, high-reliability SPA, which is very helpful in reducing the cost of mass production of AMB systems and promoting large-scale application.

4. Experimental Verification

To validate the output performance of different topologies, experiments are undertaken to compare the output current response rates. The experimental setup is shown in Figure 17. The two power supplies are employed to provide the low voltage of +15 V and +5 V and the DC bus voltage of 50 V. The load to drive is the coils of the AMB stator, whose electrical resistance and the nominal inductance are 1.6 Ω and 5.5 mH, respectively. To exclude the possible impact from different control methods, open-loop control is used to excite the electromagnet in the experiment. Additionally, the coil currents are controlled by two signal generators, RIGOL DG1022 and RIGOL DG1022U, which output PWM waves with 20 kHz frequency and corresponding duty cycle to the SPAs. The oscilloscope and current probe are implemented to observe the waveform of the coil currents.

For the experiment with half-bridge SPA, all four channels of the signal generators are applied to generate four PWM waves to control four coil currents, and the oscilloscope to record currents. The four coil currents are set to 1 A, 2 A, 3 A, 4 A, respectively, as shown in Figure 18, and the fundamental function of multi-channel drive is proven. Then, one coil current is set to 3 A, and the current rise curve is demonstrated in Figure 19. As depicted in Figure 19, it takes approximately 100 ms for the coil current to reach 3 A. The rising time in the experiment is much longer than that in the simulation, and this emphasizes the significance of closed-loop current control in practical application.

In the experiment with neutralized-sharing-bridge SPA, the SPA is modified from the existing full-bridge SPA. One phase leg of the first bridge circuit is configured as the neutralized shared phase leg, and either leg of the other bridge circuits as the legs corresponding to coils. Therefore, the coil is driven by connecting the neutralized shared phase leg and another phase leg, namely the phase leg in the first and another bridge circuit in the experiment. Four channels of the signal generators are employed to create four PWM waves, one of which is for the neutralized shared phase leg with a constant 50% duty cycle, and the other three with related duty cycles corresponding to the coil currents. The three coil currents are set to 1 A, 2 A, 3 A, respectively, as presented in Figure 20, and the neutralized-sharing-bridge SPA is confirmed to be capable of driving multiple coils. Next, one coil current is similarly set to 3 A, and the current rise curve is displayed in Figure 21. It takes about 200 ms to acquire 3 A coil current, which is twice as long as the half-bridge

SPA spends. Consequently, the experimental result is consistent with the simulation, and the advantage of half-bridge topology in output current response rate is verified.

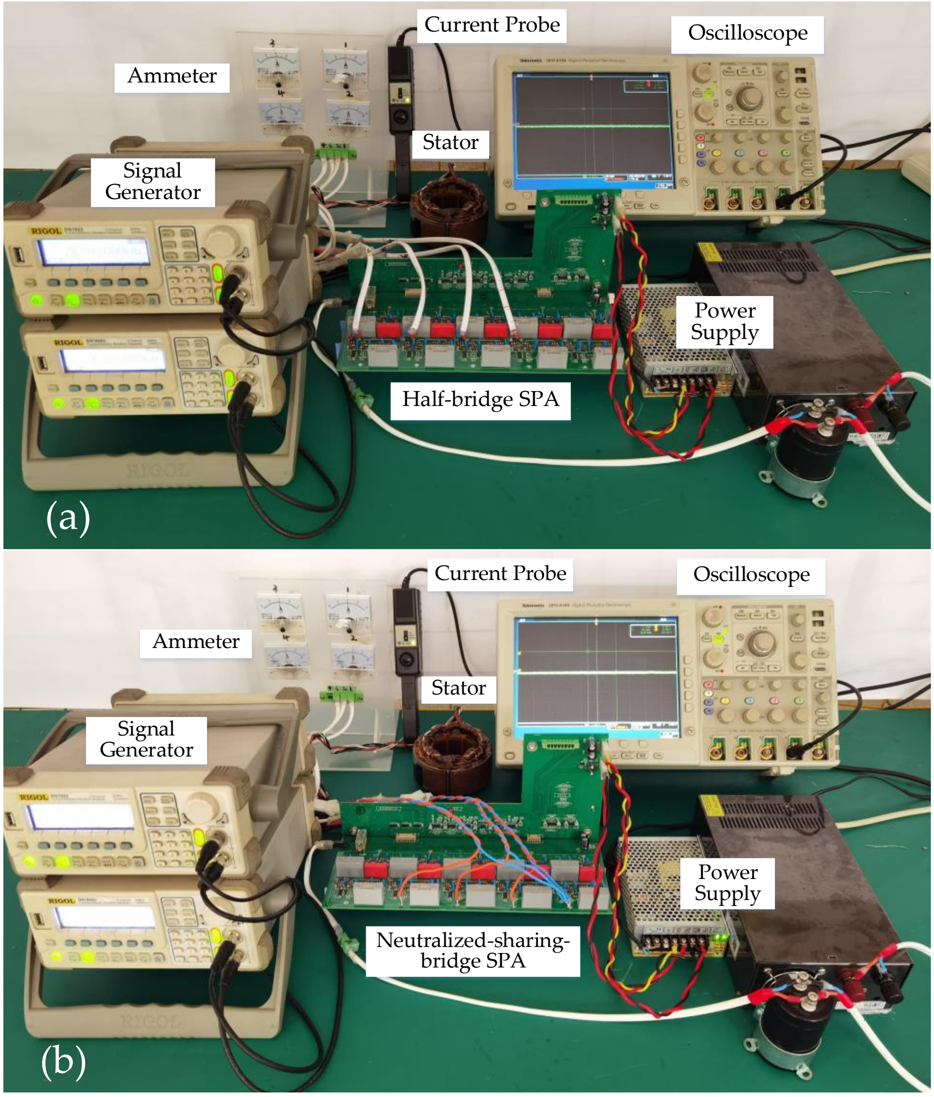

Figure 17. Experimental setup with (**a**) half-bridge SPA, (**b**) neutralized-sharing-bridge SPA.

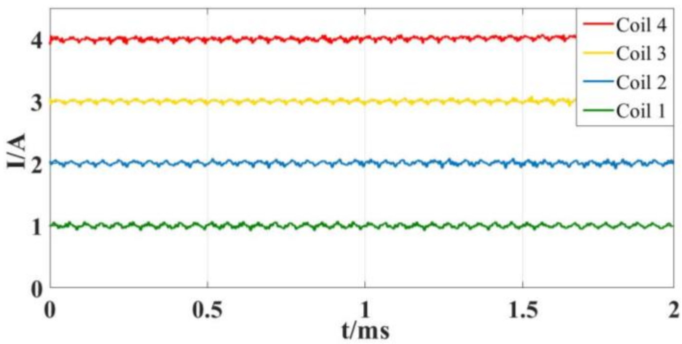

Figure 18. Coil currents driven by half-bridge SPA.

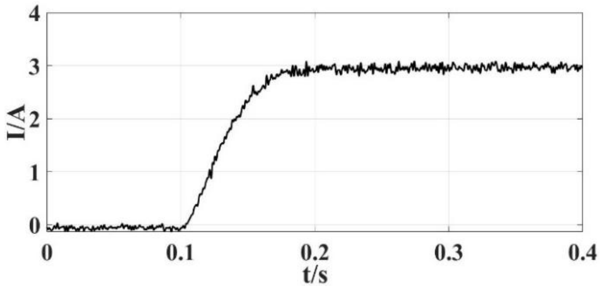

Figure 19. Current rise curve of half-bridge SPA.

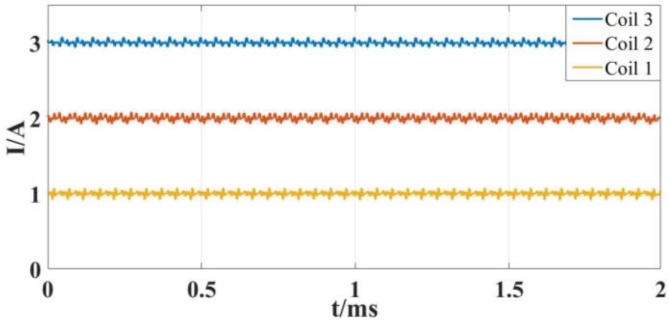

Figure 20. Coil currents driven by neutralized-sharing-bridge SPA.

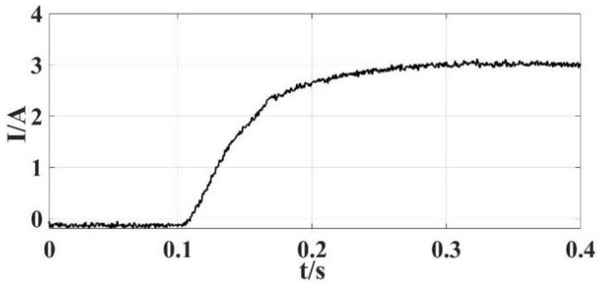

Figure 21. Current rise curve of neutralized-sharing-bridge SPA.

5. Conclusions

In this work, the SPA topology for the four DOF AMB system is discussed and evaluated. This paper mainly analyzes the traditional half-bridge topology and two novel topologies—the three-phase-half-bridge and neutralized-sharing-bridge topology—and comprehensively evaluates the volume, current output performance, and cost of the SPA; furthermore, we discuss the characteristics and application prospects of different topologies. The conclusions are as follows:

(1) The output current of SPAs with different topologies contains ripple, but the ripple can be decreased to a very low level with appropriate modulation methods;

(2) The half-bridge topology is the most traditional topology of the SPA for AMBs. Although it needs the most components and does not involve topology optimization, it has a fast output current response rate and can play an advantage in large bandwidth current control. It has wide application prospects in the control of ultra-high speed magnetically levitated rotors;

(3) The three-phase-half-bridge topology SPA controls two coils in one DOF through a three-phase-half-bridge circuit, which reduces the number of components. Even more valuable is the fact that the SPA can be directly substituted by an industrial three-phase inverter with high maturity. This topology is a priority in the industrial mass production of AMBs;

(4) Compared with the three-phase-half-bridge topology, by sharing the middle leg, the neutralized-sharing-bridge topology SPA further reduces the number of switches,

but the number of isolated drive circuits increases. Consequently, the superiority of the neutralized-sharing-bridge topology in reducing the number of components is not very apparent compared with the three-phase-half-bridge topology. However, when considering the design of the five DOF AMB system, the advantage of the high integration degree of the neutralized-sharing-bridge topology is distinct, which gives it a great application potential in aerospace and other fields with strict requirements on weight and volume.

The conclusions obtained in this paper provide theoretical guidance for the selection and design of the topology of SPAs for AMB systems in different situations, and contribute to the promotion and application of magnetic bearings in various fields.

Author Contributions: Methodology, H.W.; formal analysis, J.Z.; investigation, K.Y.; writing—original draft preparation, K.Y.; writing—review and editing, H.W. and X.G.; supervision, Y.H. All authors have read and agreed to the published version of the manuscript.

Funding: This research was funded by National Key Research and Development Project of China, grant number 2018YFB2000103.

Institutional Review Board Statement: Not applicable.

Informed Consent Statement: Not applicable.

Acknowledgments: The project was supported by National Key Research and Development Project of China with grant number 2018YFB2000103.

Conflicts of Interest: The authors declare no conflict of interest.

References

1. Chamroon, C.; Cole, M.; Fakkaew, W. Linearizing control of a distributed actuation magnetic bearing for thin-walled rotor systems. *Actuators* **2020**, *9*, 99. [CrossRef]
2. Maslen, E.H.; Schweitzer, G.; Bleuler, H.; Cole, M.; Traxler, A. *Magnetic Bearings—Theory, Design, and Application to Rotating Machinery*; Springer: Berlin/Heidelberg, Germany, 2009.
3. Xin, C.; Baixin, C.; Han, L.; Allen, G.M. An Accurate Linearization of Electromagnetic Force of Heteropolar Magnetic Bearings With Redundant Structures. *J. Eng. Gas Turbines Power Trans. ASME* **2020**, *142*. [CrossRef]
4. ISO 14839-3. *Mechanical Vibration—Vibration of Rotating Machinery Equipped with Active Magnetic Bearings—Part 3: Evaluation of Stability Margin*. Available online: https://www.iso.org/standard/39057.html (accessed on 13 June 2021).
5. Carabelli, S.; Maddaleno, F.; Muzzarelli, M. High-efficiency linear power amplifier for active magnetic bearings. *IEEE Trans. Ind. Electron.* **2000**, *47*, 17–24. [CrossRef]
6. Cheng, X.; Zhang, L.; Zhou, R.G.; Song, S.; Wang, B.; Liu, H. Analysis of output precision characteristics of digital switching power amplifier in the active magnetic bearings system. *Automatika* **2017**, *58*, 205–215. [CrossRef]
7. Chiu, H.-L.; Tsai, N.-C. Dual-mode power drive for active magnetic bearings. *IET Electr. Power Appl.* **2019**, *13*, 162–167. [CrossRef]
8. Ren, Y.; Fang, J.C. Current-sensing resistor design to include current derivative in PWM H-bridge unipolar switching power amplifiers for magnetic bearings. *IEEE Trans. Ind. Electron.* **2012**, *59*, 4590–4600. [CrossRef]
9. Fang, J.C.; Ren, Y. Self-adaptive phase-lead compensation based on unsymmetrical current sampling resistance network for magnetic bearing switching power amplifiers. *IEEE Trans. Ind. Electron.* **2012**, *59*, 1218–1227. [CrossRef]
10. Jiang, D.; Kshirsagar, P. Analysis and control of a reduced switch converter for active magnetic bearings. In Proceedings of the IEEE Applied Power Electronics Conference & Exposition, Long Beach, CA, USA, 20–24 March 2016; pp. 3616–3622.
11. Jiang, D.; Li, T.; Hu, Z.D.; Sun, H.B. Novel topologies of power electronics converter as active magnetic bearing drive. *IEEE Trans. Ind. Electron.* **2020**, *67*, 950–959. [CrossRef]
12. Zhou, J.; Deng, Z.; Liu, C.; Li, K.; He, J. Current ripple analysis of five-phase six-leg switching power amplifiers for magnetic bearing with one-cycle control. In Proceedings of the International Conference on Electrical Machines & Systems, Chiba, Japan, 13–16 November 2016.
13. Hu, Y.; Yang, K.; Guo, X.; Zhou, J.; Wu, H. Evaluation of the topology of switching power amplifiers for active magnetic bearings. *Proceedings* **2020**, *64*, 25.
14. Ran, S.; Hu, Y.; Wu, H.; Cheng, X. Resonance vibration control for AMB flexible rotor system based on mu-synthesis controller. *Math. Probl. Eng.* **2018**, *2018*, 4362101. [CrossRef]
15. Sun, J.; Zhang, Y. A novel integrated structure with a radial displacement sensor and a permanent magnet biased radial magnetic bearing. *Sensors* **2014**, *14*, 1950–1960. [CrossRef] [PubMed]
16. Kshirsagar, P.; Yan, P. Multiple-Axis Magnetic Bearing and Control of The Magnetic Bearing with Active Switch Topologies. U.S. Patent US 2015/0068243 A1, 12 March 2015.
17. Koehler, B.-U.; Denk, J.; Van Maanen, G.; Lang, M. Applying standard industrial components for active magnetic bearings. *Actuators* **2017**, *6*, 8. [CrossRef]